Biomedical Signal Processing and Control 62 (2020) 102052

Contents lists available at ScienceDirect

Biomedical Signal Processing and Control

journal homepage: www.elsevier.com/locate/bspc

Detection of time irreversibility in interbeat interval time series by visible and nonvisible motifs from horizontal visibility graph

G.I. Choudhary[a,*], W. Aziz[b,c], P. Fränti[a,d]

[a] School of Computing, University of Eastern Finland, Joensuu, Finland
[b] College of Computer Science and Engineering, University of Jeddah, Saudi Arabia
[c] Department of Computer Science & Information Technology, The University of Azad Jammu & Kashmir, Muzaffarabad, AJK, Pakistan
[d] College of Big Data and Internet, Shenzhen Technology University, Shenzhen, China

ARTICLE INFO

Article history:
Received 24 November 2019
Received in revised form 5 April 2020
Accepted 26 June 2020

Keywords:
Asymmetry measures
Graph motifs
Heart rate variability
Nonequilibrium systems
Time irreversibility

ABSTRACT

The time irreversibility is a characteristic feature of biological systems and its presence in *heart rate* (HR) is due to the complex dynamical process involved in the controlling mechanism of *cardiovascular system* (CVS). In this study, we propose a novel method referred to *time irreversibility using visibility motifs* (TIVM) for quantifying temporal asymmetry by extracting visible and non-visible *horizontal visibility graph* (HVG) motifs from a time series. The method can be applied using two simple approaches for transforming original time series into visible and non-visible motifs without mapping the time series into complex networks. *Kullback-Leibler divergence* (KLD) is used to quantify the temporal asymmetry between visible and non-visible HVG motifs of a time series. First, we explore the structural relation between HVG motifs and ordinal patterns reveal that motifs with different structures can have the similar visibility level. Next, we apply the method to find the asymmetry in different synthetic signals and real world *interbeat interval* (IBI) time series from healthy and pathological subjects. The findings reveal that the proposed method provide more accurate information about the healthy biological systems and changes occurring due to aging or disease. It is an effective tool for discriminating healthy young, elderly and pathological groups.

1. Introduction

Beat-to-beat variations in the heart rate called *heart rate variability* (HRV) is a physiological phenomenon involved in the *cardiovascular system* (CVS) regulatory mechanism [1]. The healthy CVS exhibits nonlinear behavior due to interaction of many feedback loops revealing that dynamics of output signals are complex in nature [1–4]. Thus, nonlinear complexity measures such as time irreversibility [3,5–8] and entropy based measures [9–12] are more suitable to quantify the dynamical information encoded in the *interbeat interval* (IBI) time series for detailed description of CVS controlling mechanism of the healthy subjects and changes occurring due to aging and disease.

Time irreversibility is a characteristic feature of nonequilibrium systems, and it refers to the lack of invariance of the statistical properties extracted from a biological signal under the operation of time reversal [7,13]. It is present in different biological systems ranging from the cellular levels to the system levels [14]. The physiological system utilizes energy to evolve structural configurations that helps them to adopt surrounding environment [10]. The capability to adapt to a dynamic environment is directly related to the unidirectionality of the energy flow across the system's boundaries, hence the irreversibility of the underlying processes [7,10]. Aging and diseases decrease the capability of self-organizing and adopting of a biological system to adopt dynamical environment, which is associated with the loss of time irreversibility. The presence of time irreversibility in heart rate signal is due to the complex dynamic process involved in the controlling mechanism of CVS [15]. Thus, CVS controlling mechanism is intrinsically complex, functioning far from equilibrium having self-organizing and adapting capability in healthy conditions [7].

Numerous time irreversibility indices have been proposed and applied to human IBI time series to quantify heart rate asymmetry in healthy and disease groups [2,7,8,10,16]. Porta et al. [2] examined the asymmetry of a Poincaré plot and explored the interrelationship between time reversibility, pattern asymmetry and nonlinear dynamics using three asymmetry indices, Guzik's index [6], Porta's index [16] and Ehlers' index [5]. The main limitation of these traditional measures is that they operate on single time scale whereas the integrative behavior of a biological system appears at multiple

* Corresponding author.
E-mail address: gulraiz@cs.uef.fi (G.I. Choudhary).

https://doi.org/10.1016/j.bspc.2020.102052
1746-8094/

time scales. This is a major source for the inaccuracy of the traditional methods. Costa et al. [7] solved the problem by proposing multiscale time irreversibility measure, which provides more useful insight of different situations in patients with coronary heart disease and healthy subjects of the same age [7,10]. While working reasonably well, the method requires relatively long and stationary signal to process it at multiple time scales [7], which increases the time complexity.

Lacasa et al. [17,18,26,27,29] proposed a computationally more efficient method by combining *horizontal visibility graph* (HVG) algorithm and the *Kullback-Leibler divergence* (KLD). This approach maps a time series to a directed visibility graph according to a geometric criterion, and then uses KLD to estimate the degree of irreversibility between the in and out *degree distributions* (DD) of the associated graph. However, the degree distribution is unreliable because two networks can have exactly the same degree distribution even if their local structure would be completely different [19].

Flanagan and Lacasa [20] extended and studied the concept of time irreversibility to the context of financial time series using this approach and findings revealed that the stock prices of the companies are time irreversible. However, performance of this approach is modest in discriminating healthy and pathological IBI time series data (refer to Table 3). Martinez et al. [21] proposed a novel time irreversibility index based on the ordinal pattern analysis. The research demonstrated the applicability and advantages of the index by many examples from, synthetic and real, linear and nonlinear models. To date, time irreversibility methods employed to evaluate the complexity of physiological time series either cannot discern accurate dynamical information or have poor discrimination power.

In this study, we propose a novel approach called *time irreversibility from visibility motifs* (TIVM) to analyze temporal asymmetry by extracting visible and non-visible HVG motifs. We use a visibility measure to generalize the HVG approach that identifies the changes in the sequence as visible, otherwise non-visible. Both visible and non-visible sequences accommodate different structures. The fluctuations in the time series data give rise to visible structures, whereas the data points which are monotonically increasing or decreasing result into non-visible structures. We utilize ordinal patterns and HVG patterns to find the different structures falling under visibility and non-visibility structures. Furthermore, TIVM computes the distance between the visible and non-visible distribution of a time series.

We apply the proposed measure to find the asymmetry in different synthetic and real time IBI time series of healthy and pathological subjects. We compare the performance of TIVM with several time irreversibility indices in terms of dynamical information and discrimination power for distinguishing IBI time series of *normal sinus rhythm young* (NSRY), *normal sinus rhythm elderly* (NSRE), *congestive heart failure* (CHF), and *atrial fibrillation* (AF) subjects. The compared indices include *Porta's index* (PI), *Guzik's index* (GI), and *multiscale entropy* (MTI). The results show that TIVM and MTI reveal dynamical information more accurately than traditional irreversibility indices. TIVM outperforms all time irreversibility measures in discriminating between NSR young vs NSR elderly (AUC = 0.77), NSR vs CHF (AUC = 0.93) and NSR vs AF (AUC = 0.98) while the second best measure, multiscale time irreversibility, discriminate NSR young vs NSR elderly (AUC = 0.73), NSR vs CHF (AUC = 0.89) and NSR vs AF (AUC = 0.95). We also compare the results of TIVM with our previous study [9] in terms of procedural differences, classification ability and the aspect of complexity the measures quantify.

2. Data

To evaluate the performance of TIVM, we use synthetic signals and clinical time series datasets.

2.1. Synthetic data

Synthetic data comprises of 40 realizations of simulated noise signals including *white Gaussian noise* (WGN) and $1/f$ noise signals, and chaotic map time series each with 30,000 data points. WGN is randomly drawn from a Gaussian distribution and statistically uncorrelated signal with constant power spectral density $S(f)$. It is defined as follows:

$$S(f) = \frac{C_w}{|f|^0} \tag{1}$$

where C_w is a constant [22]. In case of $1/f$ noise, the power spectral density is inversely proportional to the frequency and equals to the amount of energy octave, whose power spectral density is as follows:

$$S(f) = \frac{C_f}{|f|^a} \tag{2}$$

where C_f is a constant and a can be changed between 0 and 2. The $1/f$ noise was generated by taking the fast Fourier transform of uniformly distributed white noise and then after imposing $1/f$ distribution on the power spectrum, inverse Fourier transform was computed. It can be seen from Eq. 2 that the power spectrum density of pink noise is inversely proportional to frequency [22]. Therefore, the pink noise is more complex than WGN, due to the presence of long-range correlations.

The chaotic maps dataset consists of logistic map and Henon map. The logistic map is quadratic function that exhibits the chaotic behavior and is mathematically written as:

$$x_{n+1} = rx_n(1 - x_n) \tag{3}$$

where x_n represent the ratio of existing population to maximum possible population. It varies between 0 and 1, and the value of the parameter $r \in [0,4]$. We used same ranges from 0.01–4 as in [23] at different initial values of x_n of logistic map time series. The Henon map is a discrete time dynamical system and is two-dimensional extension of logistic map and mathematically written as:

$$\begin{cases} x_{n+1} = y_n + 1 - ax_n^2, \\ y_{n+1} = bx_n. \end{cases} \tag{4}$$

where $a = 1.4$ and $b = 0.3$. For experiments, we generated 30 synthetic signals, each comprised of 30,000 data points.

2.2. Clinical data

The clinical dataset we used in our study is a combination of 4 datasets obtained from Physionet [24]. The data consists of IBI time series signal of 140 subjects. A detail summary of the dataset is shown in Table 1. It consists of 72 healthy, 44 congestive heart failure, and 24 atrial fibrillation subjects. The data of healthy subjects is obtained using 24 -h Holter monitor recording and divided into healthy young (NSRY< = 55) and healthy elderly (NSRE > 55).

The IBI time series data of 44 congestive heart failure were obtained from 24 -h Holter monitor recordings. 29 out of 44 were taken from the IBI congestive heart failure database and remaining 15 from MIT-BIH Bidmic *congestive heart failure* (CHF) database. Based on *New York Heart Association* (NYHA) classification, the CHF

Table 1
Details of the Physionet Datasets: 72 healthy subjects from MIT-BIH normal sinus rhythm database, 44 CHF subjects from RR-Interval congestive heart failure database and MIT-BIH Bidmic congestive heart failure, 24 AF subjects from MIT-BIH atrial fibrillation database.

	NSRY	NSRE	CHFA	CHFB	AF
Total Subjects	26	46	12	32	24
Gender	10 M 16 F	25 M 21 F	12 Unknown	19 M 6 F 7 Unknown	Unknown
Age Group	20–55	>55	20–78	20–78	20–78
Recorder	24 h Holter Monitor	24 h Holter Monitor	24 h Holter Monitor	24 h Holter Monitor	10 h Ambulating ECG Recorder
Sampling Frequency	128 Hz	128 Hz	128 Hz	17 128 Hz 15 MIT BIH 250 Hz	250 Hz

Table 2
Horizontal visibility graph motifs and frequencies extracted from time series data of 20 points.

Motifs	Type	Frequencies
	Non-visible	6
	Visible	4
	Visible	6
	Visible	1
	Visible	0

subjects are divided into 4 classes, which further divided into two groups using a functional classification system. The class I and II are in the *congestive heart failure A* (CHFA) group, and class III and IV are in the *congestive heart failure B* (CHFB) group [25].

The atrial fibrillation dataset of 24 subjects is also obtained from MIT-BIH atrial fibrillation database. The recording duration of atrial fibrillation subject is 10 h. The ambulatory electrocardiogram recorder used to record analogue signal using a bandwidth of approximately 0.1 Hz–40 Hz and 250 Hz sampling frequency.

3. Method

3.1. Horizontal visibility graph motifs

Given a time series $\{x_n\}^N{}_{n=1,2,\ldots N}$, comprising of N interest intervals we generate patterns as follows. Consider a sliding window of size m, the time series is converted into $N-m+1$ patterns P, using the relation

$$P_m(k) = \begin{bmatrix} x_1 & x_2 & \ldots & x_m \\ x_2 & x_3 & \ldots & x_{m+1} \\ \vdots & \vdots & \ldots & \vdots \\ x_{N-m+1} & x_{N-m+2} & \ldots & x_N \end{bmatrix}, \forall 1 \le k \le N-m+1$$

Consider a time series of x_n = {0.69, 0.71, 0.71, 0.70, 0.71, 0.68, 0.69, 0.66, 0.68, 0.65, 0.67, 0.68, 0.71, 0.70, 0.72, 0.71, 0.71, 0.71, 0.73, 0.69} comprising of N = 20 data points as shown in Fig. 1.

The HVG algorithm transforms each data point x_i into a vertex in the graph. Two vertices i and j are connected if the following geometrical criteria within the sliding window is fulfilled:

$$\min(x_i, x_j) > x_m \, \forall x_m : i < m < j \tag{5}$$

Using Eq. (5), we get the horizontal visibility graph (shown in Fig. 2) from IBI time series data similarly as in [9]. Next, we use sliding window of size m = 4 to extract all possible motifs of size m from the time series. All motifs, their types and frequencies are listed in Table 2. The frequencies show that visibility motifs occurs more frequently than non-visible motifs.

The motifs of the horizontal visibility graph form the group of patterns having similar geometrical symmetries as shown in Figs. 3 and 4. The patterns with monotonically increasing or decreasing order or with steady values are perceived as non-visible (Fig. 3), whereas patterns with changes are perceived as visible. Extraction of visible and nonvisible motifs can be helpful for understanding dynamical information encoded in the physical and physiological systems. However, the process of motif extraction by transforming time series into HVG is a time-consuming task. Thus, extracting visible and non-visible motifs without transforming time series into HVG is crucial for quantifying dynamical information in real-time.

3.2. Visible and non-visible patterns

In order to simplify the horizontal visibility method and to find the structural asymetry between visible and non-visible motifs, we propose two metods that can extract visible and non-visible motifs without transforming time series into HVG.

Method 1: To extract *non-visible* (NV) and visible motifs in HVG, we define a criterion to find the index of the largest and second largest motifs using a sliding window. The two data points are visible if one can draw a horizontal line in the time series joining i and j which does not intersect any intermediate data. Hence i and j are two visible nodes if the following criterion is fulfilled within the sliding window. The binary transformation is used to generate visible and non-visible patterns.

$$Motif = \begin{cases} Visible, & if\ (firstLargest_{index} - secondLargest_{index}) > 1 \\ Nonvisible, & otherwise \end{cases} \tag{6}$$

Method 2: The second method to extract the visible and non-visible motifs comprises of the following steps.

Step 1: Compute the first differential of the time series

$$\Delta x(i) = x_{i+1} - x_i,\ i\varepsilon\,[N-1].$$

Step 2: Transform Δx into a sign series using the criteria

$$Sx(i) = \begin{cases} 1, & \Delta x \ge 0 \\ 0, & otherwise \end{cases}$$

Step 3: The random values of $s(x)$ and structure order ending with zero reveals the frequent changes in the pattern, whereas order in the patterns reveals monotonically increasing and/or decreasing patterns within the window size. Starting from n = 2 to N, sign change (SC) series is generated as

$$SC(i) = n,\ if\ Sx(n) \ne Sx(n+1)\ i\varepsilon[1,\ M+1]$$

where M is the total number of sign changes in the Sx series and i runs from 1 to M. $SC(i)$ will always be a non-decreasing function of i.

Step 4: The visible and non-visible motifs are determined using the SC series as follows.

$$Motif = \begin{cases} Nonvisible, & SC(i) \ne 0 \vee SC(i) \ne 1]) \\ Visible, & otherwise \end{cases}. \tag{7}$$

The two data points are not visible if there is a consecutive sequence of zeros and ones. Otherwise it validates that horizontal visibility is present.

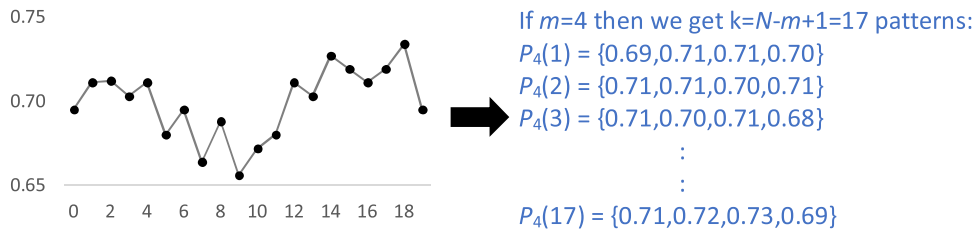

Fig. 1. IBI time series of 20 data points and patterns extracted using overlapping window of size 4.

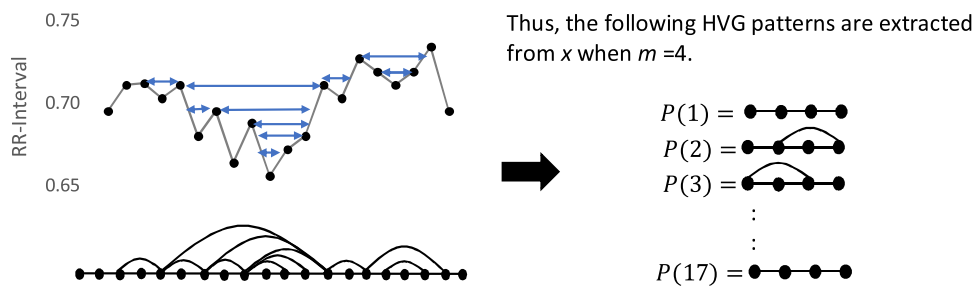

Fig. 2. Illustrative example showing the horizontal visibility indicated by arrows, mapped on time series of 20 data points (left-top), the extracted Horizontal visibility graph (left-bottom), and the motifs extracted from these patterns (right).

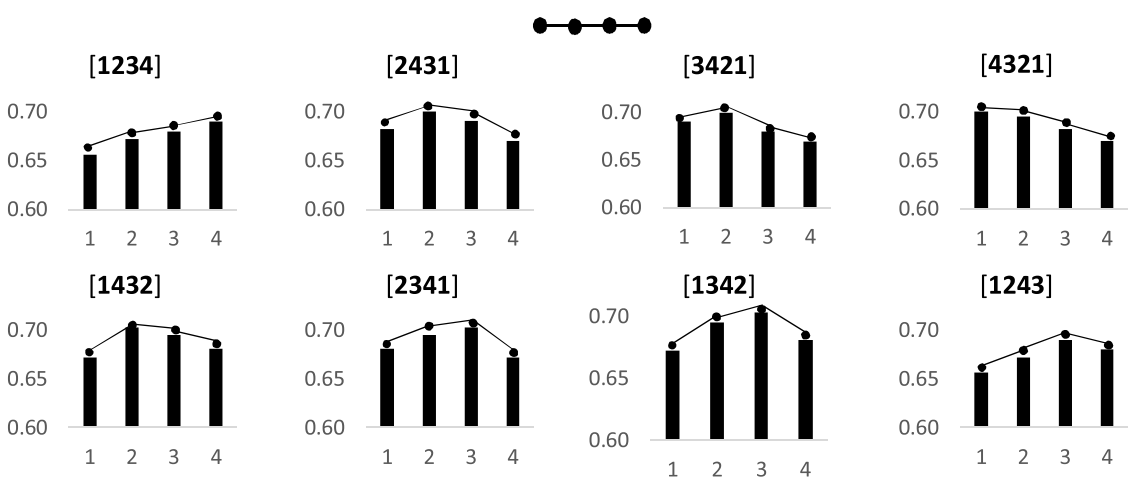

Fig. 3. The structural relation between the ordinal patterns and non-visible graph motifs for window size = 4.

3.3. Quantification of time irreversibility using KLD

To quantify time irreversibility, we first calculate the probability of occurrence of visible (P_v) and non-visible (P_{nv}) motifs:

$$P_v(m) = \frac{n_v(m)}{N-m+1} \tag{8}$$

$$P_{nv}(m) = \frac{n_{nv}(m)}{N-m+1} \tag{9}$$

where, $n_v(m)$ is the number of visible and $n_{nv}(m)$ the number of non-visible patterns. *Kullback-Leibler divergence*, also known as *relative entropy*, is used as a measure to calculate the distance between two distributions. In specific, we apply KLD to measure the distance between the distribution of visibility and non-visible motifs:

$$KLD\ (x, m) = \sum_i P_v(m) \log\left[\frac{P_v(m)}{P_{nv}(m)}\right] \tag{10}$$

Proceeding with the example given in Table 2, we derive the probabilities of visible motifs $P_v(4) = 6/17 = 0.353$, and the probability of non-visible motifs $P_{nv}(4) = 11/17 = 0.65$. Applying KLD, we get $KLD(x, 4) = 0.35\, log\,(\frac{0.35}{0.65}) = 0.09$. The process is irreversible if the value obtained is higher than 0, otherwise reversible. Values close to 1 depicts higher degree of time irreversibility.

3.4. Statistical analysis

Statistical analysis is performed using *variance* (ANOVA) analysis to find the differences among group means. The one-way ANOVA is based on significant F-statistics that calculate the ratio of variance among the means to the variance within the groups and determines statistical difference among the different group means. The results are considered statistically significant at significance level $p \leq 0.05$. The ANOVA test only determines that there is a statistically significant difference between group means, but it does not show which groups differ from each other. The Bonferroni post-hoc test is generally the preferred test for paired comparison of groups.

Receiver operator characteristic (ROC) curve is used in evaluating the performance of a technique to discriminate between healthy and pathological groups. *Area under ROC curve* (AUC) is a quantitative index describing this curve [30]. In this study, we

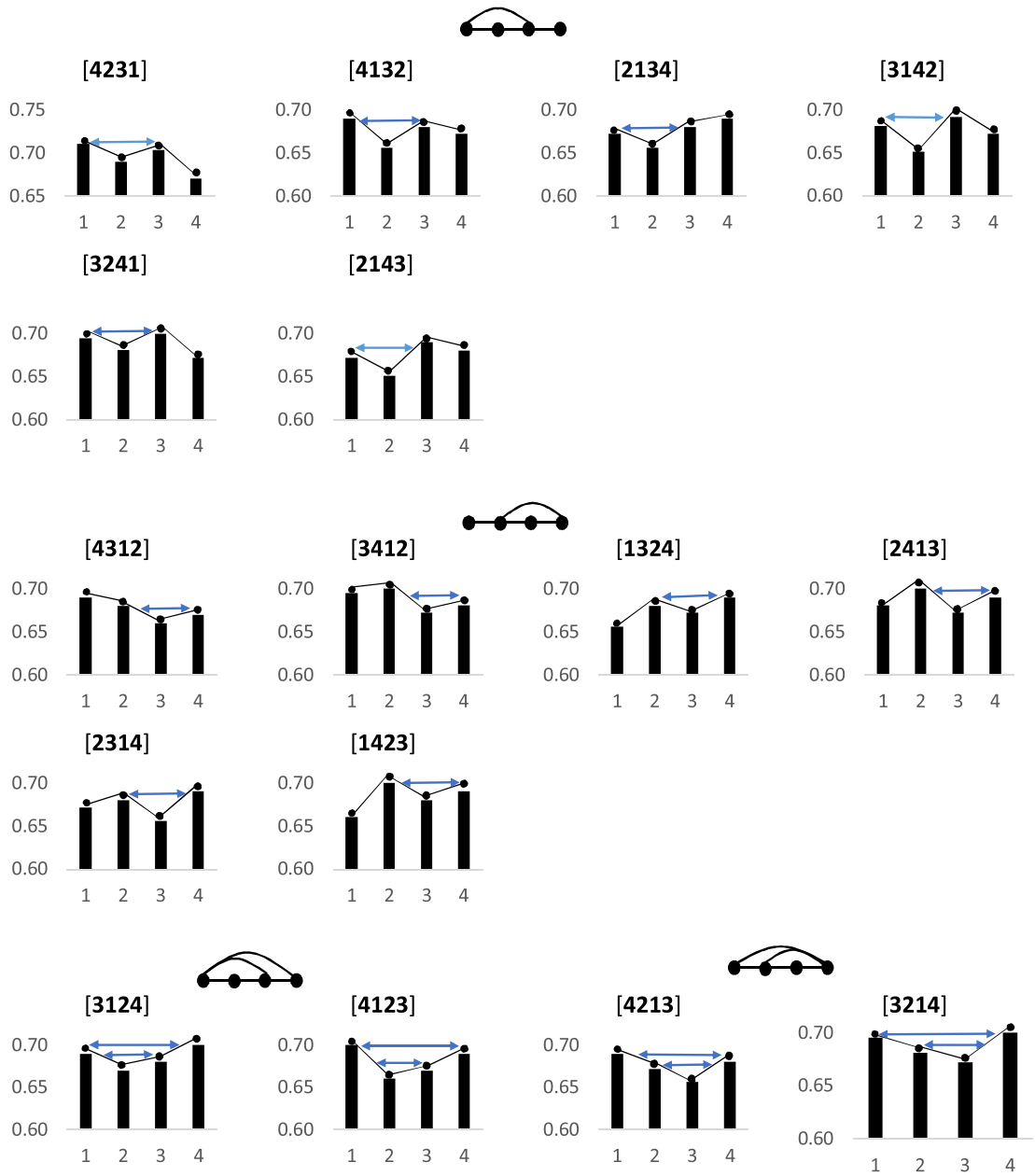

Fig. 4. The structural relation between ordinal patterns and visibility graph motifs.

use AUC as a measure of diagnostic performance to discriminate between healthy and pathological groups for performance evaluation of TIVM with other time irreversibility measures. An area of 1 represents 100 % separation between two groups, whereas an area of 0.5 means the less chance of discrimination between the groups.

4. Results

We compare the performance of the proposed method to compute HVG patterns that allows to extract visibility and non-visibility motif at different window sizes. The time irreversibility of visible and non-visible motifs is quantified using KLD.

4.1. Synthetic signals

We first evaluate the performance of the method for synthetic signals: simulated noise signals and chaotic time series data. Fig. 5 shows the result of TIVM using different window size for discriminating simulated noise signals (WGN and $1/f$ noise) on left, and chaotic time series of logistic and henon maps on right.

From the Fig. 5, it is evident that at window sizes smaller than 6, TIVM either provides dynamically incorrect information or show poor separation between simulated noise signals. However, at window sizes 6 and above, the values of TIVM are higher for $1/f$ noise than for WGN. The $1/f$ noise signals are dynamically more complex than WGN due to presence of long-range correlations [9,31]. Higher values of TIVM reveal that $1/f$ noise signals are more time irreversible, which is an important characteristic of complex systems. Maximum separation between the two noise signals is obtained at window size 8. Similarly, for chaotic time series data of logistic and henon maps, TIVM provides dynamically incorrect information at smaller widow sizes. However, dynamically accurate information is obtained at window sizes 6 and above. The reason is that logistic map time series is dynamically more complex than henon map.

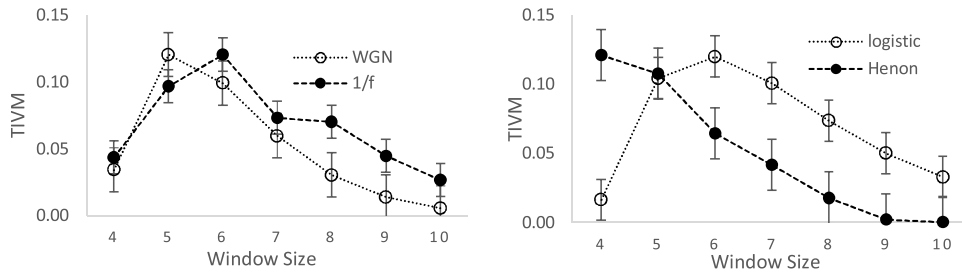

Fig. 5. Mean ± standard deviation of TIVM for synthetic data at different window sizes. Left: simulated noise signals; Right: chaotic time series data at different window sizes.

4.2. Interbeat interval time series data

To test the effectiveness of TIVM to classify the real time series, we applied it on interbeat interval time series of NSR and CHF subjects under different physiological and pathological conditions. We examined the changes occurring due to disease and aging. In Fig. 6, the results of TIVM for distinguishing NSRY vs NSRE, NSRY vs CHFA, NSRY vs CHFA and NSRY vs AF subjects at different window sizes are shown. Higher values of TIVM reveal higher time irreversibility, which characterizes that their system dynamics are complex. The symbols represent mean values and the error bars represent standard deviation. We evaluated the performance of proposed method at different window sizes, dynamically accurate and better separation between groups was found at window sizes seven and above. It is evident that TIVM is higher for NSRY than for NSRE, CHFA, CHFB and AF subjects at window sizes 7 and above, revealing that healthy young subjects exhibit higher complexity compared healthy elderly and pathological subjects. The results highlight that TIVM shows significant difference between NSRY vs NSRE, NSRY vs CHFA, NSRY vs CHFB as well as NSRY and AF subjects at these window sizes.

In Table 3, mean ± Standard deviation of TIVM estimates at optimal window size for separating NSRY, NSRE, CHF and AF subjects are shown. The results are statistically significant if the significance level is less or equal to 0.05. AUC is used as a measure of degree of separation between the groups. The findings of the proposed technique (TIVM) are compared with time irreversibility measures MTI, TiROP, Guizk's index, Porta's index and degree distribution approach in terms of accurate dynamical information and discrimination power. It is evident from the table, TIVM and MTI are the only two irreversibility measures that provide dynamically accurate information; higher irreversibility for NSRY compared to elderly and pathological groups. The proposed technique validates the loss of complexity (time irreversibility) with aging and disease hypothesis. TIVM outperforms all the previously developed time irreversibility measures for distinguishing NSRY vs NSRE, NSRY vs CHF, and NSRY vs AF followed by MTI.

4.3. Sensitivity with signal length

We tested the sensitivity of TIVM with signal length using IBI time series data of healthy and pathological subjects for data lengths 1000, 2000, 5000, 10000, 20,000 and 30000. It is evident from Fig. 7, TIVM values remain almost same at all data lengths for specific healthy and pathological group. Results reveal that TIVM values do not vary with data length and can be used for the analysis of both short and long duration signals.

4.4. Robustness in the presence of outliers

In IBI time series, recording artefacts and missed beats are two outliers. To test the robustness of TIVM in the presence of outliers, we used IBI time series data of NSR subjects with and without (Fig. 8a) outliers. We used 30,000 data samples of IBI time series of an NSR subject. In this data there are 209 outliers (0.69 %) having values greater than 2 s. Due to their smaller number, these outliers were excluded from the IBI time series. Fig. 8a shows the results of TIVM for the unfiltered and filtered IBI time at different window size. We found an overlap of the TIVM values for the filtered and unfiltered time series at different window sizes. The results indicate that the proposed method is robust, even in the presence of a small percentage of high amplitude outliers.

We also determine the effect of different percentages of outliers on TIVM values (Fig. 8b). For this purpose, we use time series data of NSR subjects and added outliers in the range of 1–5 percent. It is evident from Fig. 8b that small percentage of outliers does not affect the TIVM values at all window sizes. For higher percentage of outliers, TIVM values decrease with the increase in the percentage of outliers at window size 4, whereas increasing the window size beyond 4 showed an increase in the overlap. At the window size 7, the original and noise percentages almost overlap. However, increasing the window size beyond 7 resulted in the decrease in the overlap of the TIVM for higher percentage of outliers. The results demonstrate that TIVM is robust to the presence of small percentage of outliers at all window sizes, however for higher percentage of outlier window size 7 is robust.

4.5. Comparison of TIVM and GHVE

The difference between our previous [9] and current study can be highlighted in terms of procedural details, classification ability and the aspect of complexity these measures quantify. The computation of grouped horizontal graph entropy (GHVE) [9] comprises of two steps. First, we transform the time series into HVG motifs and group them on the basis of number of edges. Next, we compute the probability of occurrence of the grouped motifs and use Shannon entropy to quantify complexity. On the other hand, TIVM is computed by transforming time series into visible and non-visible HVG motifs. Transformation of time series into HVG graph and extracting HVG motifs is a time consuming task. We simplify the horizontal visibility method and proposed two simple approaches to extract visible and non-visible motif without transforming time series into HVG. After this, we computed the probability of occurrence motifs and used KLD to quantify temporal asymmetry of the time series.

We compare the results of TIVM with GHVE for distinguishing health, pathological and elderly subjects. It is evident from Table 4 that both measures performed almost equally in distinguishing NSRY and CHF subject, TIVM outperformed GHVE in sperating NSRY and AF subjects, whereas GHVE was robust in distinguishing NSRY and NSRE. The TIVM has the additional advantage that it can be used for short duration signals. Furthermore, GHVE quantifies the information content of a signal across different window sizes, whereas

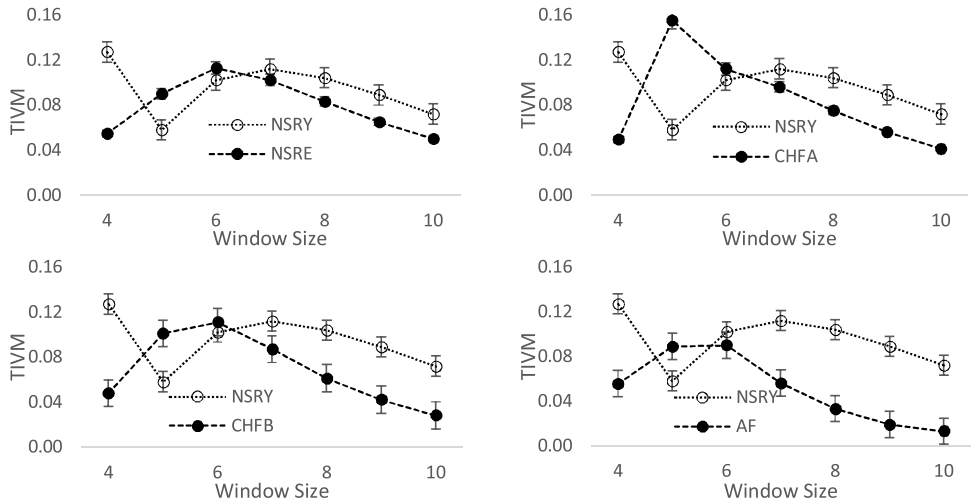

Fig. 6. Mean ± Standard deviation of TIVM estimates at optimal window size and its comparison with MTI, TiROP, Guizk's index, Porta's index and degree distribution approach for separating NSRY, NSRE, CHF and AF subjects are shown.

Table 3
Comparison of TIVM, Multi scale, Guzik Index, porta index and degree distribution for distinguishing NSRY, NSRE, CHF and AF subjects. areas under ROC (AUC) for optimal separation between healthy, low disease severity and high disease severity (AUC = 0.5 is equivalent to simple guessing and AUC = 1 is equivalent to perfect separation between classes, P-VALUE shows significant difference at ≤ 0.05).

	Mean ± Standard Error				NSRY VS NSRE		NSRY VS CHF		NSRY VS AF	
	NSRY	NSRE	CHF	AF	p-value	AUC	p-value	AUC	p-value	AUC
TIVM	0.07 ± 0.00	0.04 ± 0.00	0.03 ± 0.00	0.01 ± 0.00	3.40×10^{-3}	0.77	1.51×10^{-8}	0.93	4.01×10^{-9}	0.98
MTI [7]	0.41 ± 0.04	0.26 ± 0.03	0.15 ± 0.02	0.10 ± 0.02	1.20×10^{-3}	0.73	4.79×10^{-7}	0.89	3.90×10^{-8}	0.95
TiROP [21]	0.10 ± 0.04	0.08 ± 0.05	0.09 ± 0.05	0.05 ± 0.03	0.07	0.66	0.45	0.61	3.50×10^{-3}	0.81
Guzik Index [6]	3.69 ± 0.57	6.64 ± 0.65	5.00 ± 0.88	4.13 ± 0.67	1.10×10^{-3}	0.70	0.49	0.55	0.76	0.53
Porta Index [16]	1.45 ± 0.19	1.15 ± 0.19	1.66 ± 0.49	2.79 ± 0.57	0.70	0.63	0.08	0.63	0.61	0.53
DD [18]	0.01 ± 0.00	0.01 ± 0.00	0.02 ± 0.01	0.03 ± 0.02	0.04	0.65	0.19	0.60	0.98	0.50

Table 4
Comparison of TIVM with GHVE for distinguishing NSRY, NSRE, CHF and AF subjects. areas under ROC (AUC) for optimal separation between healthy, low disease severity and high disease severity (AUC = 0.5 is equivalent to simple guessing and AUC = 1 is equivalent to perfect separation between classes, P-VALUE shows significant difference at ≤ 0.05).

	Mean ± Standard Error				NSRY VS CHF		NSRY VS AF		NSRY VS NSRE	
	NSRY	NSRE	CHF	AF	p-value	AUC	p-value	AUC	p-value	AUC
TIVM	0.07 ± 0.00	0.04 ± 0.00	0.03 ± 0.00	0.01 ± 0.00	1.51×10^{-8}	0.93	4.01×10^{-9}	0.98	3.40×10^{-3}	0.77
GHVE [9]	3.15 ± 0.02	2.95 ± 0.02	2.83 ± 0.03	2.88 ± 0.04	9.65×10^{-13}	0.94	1.10×10^{-8}	0.91	6.27×10^{-7}	0.89

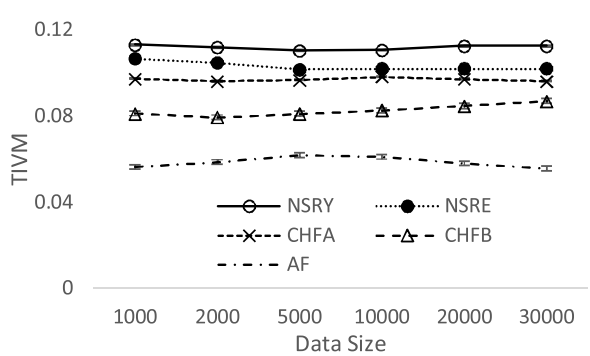

Fig. 7. Sensitivity of TIVM with signal length using IBI time series data of healthy and pathological subjects for data lengths of 1000 to 30,000 samples.

TIVM quantifies the degree of temporal irreversibility using visible and non-visible HVG notifs. Thus, GHVE and TIVM quantify different aspects of complexity and are therefore independent of each other.

5. Discussion

In this paper, we have introduced a method to measure the time irreversibility of real valued nonstationary stochastic time series. The algorithm uses two alternative approaches for extracting visible and non-visible graph patterns without transforming time series data into horizontal visibility graph. In this way, we extract pattern distribution from the original time series that enables us to study the statistical properties of motif distributions. To calculate time irreversibility of a time series, the Kullback-Leibler divergence is used to measure the distance between the visibility and non-visibility distribution. If the obtained value is greater than 0, it shows the time series is irreversible.

The method has been validated by studying the simulated (WGN, $1/f$, chaotic logistic and henon maps) time series data. The method not only discriminates but also quantifies the amount of irreversibility present in the series as it shows the amount of structural difference on $1/f$ noise as compare to WGN. The findings reveal that $1/f$ noise signals are more time irreversible than WGN. Higher time irreversibility is an indicator of higher complexity of the underlying system.

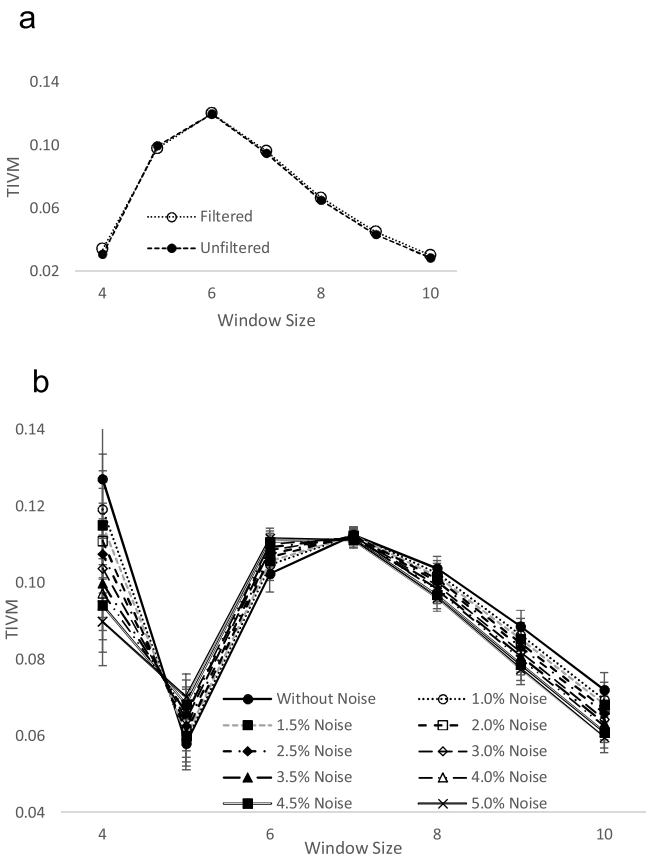

Fig. 8. a) Temporal asymetry analysis of interbeat interval time series of healthy subjects before and after removing outliers greater than 2 s (on top). b) Temporal asymetry analysis of interbeat interval time series of healthy subjects after adding different percentage of random artefacts.

The findings are inline with numerous studies which aver that $1/f$ noise signals are dynamically more complex than WGN due to the presence of long range correlations [9,28]. The analysis results of TIVM conducted on the chaotic time series data unveiled that logistic map time series are more complex than Henon time series.The overlap of TIVM values for filtered and unfiltered time series at different windows reveals the robustness of the proposed approach for extracting accurate information in the presence of dynamical or observational noise. When the method is applied on different lengths of time series, it maintained high power of discrimination on both smaller and larger length of time series. There were no significant difference in relation to the number of IBI intervals indicating no systematic differences in their values in relation to data length.

To test the hypothesis that cardiac interbeat of healthy subjects are more time irreversible than pathological subjects, we applied TIVM on healthy young, healthy elderly and pathological (CHF and AF) subjects. The results indicated that TIVM is not only discriminate accurately between healthy and diseased groups, but also provided dynamically accurate information about underlying system dynamics. We found higher time irreversibility in healthy young subjects, which decreased for the elderly and pathological subjects.

The dynamics route of cardiac problems change the struture of IBI time series in two ways [15]. The CHF, is associated with loss of variability (generation of more regular patterns), whereas for AF it is associated with substantial variability (random pattern) in the IBI time series. Depsite of different dynamical structure of CHF and AF time series, TIVM revealed decrease in time irreversiblity compared to healthy subjects. This elucidates that dynamics of healthy subjects are more time irreversible than pathological subjects. Thus, loss of time irreversibility is the generic feature of disease. The values were also higher for healthy young followed by healthy elderly, CHF and AF respectively. The results are inline with the study [10], that loss of time irreversibility aging and disease is a marker of broken heart rate asymmetry. The onset diseases decrease the self-adaptive capbility.

The outcomes of the present study can be gauged in terms of accurate dynamical information and classification ability as compare to previously developed time irreversibility measures. Regarding the dynamical information, TIVM and MTI are the only measures which provide dynamically accurate information so that healthy subjects exhibit higher time irreversibility, whereas aging and disease are associated with loss of time irreversiblity. All other time irreversibility measures, including TiROP, Guzik's index, Porta's index and degree distribtion failed to reveal accurate dynamical information. TIVM outperformed all other time irreversibility measures in classifying NSRY & NSRE, NSRY & CHF, and NSRY & AF subjects.

6. Conclusion

In this study, we propose a novel time irreversibility index TIVM to address the problem of assessing temporal asymmetry using horizontal visibility graph motifs. The proposed method extracts the temporal sequences from the original time series that allows to study the statistical difference between the visibility and non-visibility motif distributions. The time series is reversible if the interaction between the patterns is similar, whereas a significant difference in the interaction between the patterns shows that the time series is irreversible. When TIVM was applied on both synthetic and human interbeat interval time series data, we found that TIVM has higher discrimination power to distinguish correlated and uncorrelated signals, but it also tells the amount of asymmetry in both signals. To validate the performance of TIVM, we compared it with other known methods for distinguishing interbeat interval time series of healthy and pathological subjects. The results show that TIVM is a better measure to quantify the dynamics accurately and outperformed other measures for distinguishing healthy and pathological subject. Furthermore, TIVM is robust in the presence of outliers and different signal lengths.

Author contribution statement

G. I. C. and W. A. conceived of the presented idea. G. I. C. developed the theory and performed the computations. W. A. and P. F. verified the analytical methods. The principal authors writing paper were G. I. C. and W. A.. All authors discussed the results and helped shape the research, analysis and manuscript.

Declaration of Competing Interests

The authors declare that they have no known competing financial interests or personal relationships that could have appeared to influence the work reported in this paper.

References

[1] T. Force, Standards of measurement, physiological interpretation and clinical use. Task force of the European Society of Cardiology and the North American Society of Pacing and Electrophysiology, Circulation 93 (5) (1996) 1043–1065.
[2] K.R. Casali, et al., "Multiple testing strategy for the detection of temporal irreversibility in stationary time series,", Phys. Rev. E 77 (6) (2008) 66204.
[3] M. Javorka, Z. Turianikova, I. Tonhajzerova, K. Javorka, M. Baumert, The effect of orthostasis on recurrence quantification analysis of heart rate and blood pressure dynamics,", Physiol. Meas. 30 (1) (2008) 29.

[4] L. Chladekova, Z. Turianikova, I. Tonhajzerova, A. Calkovska, M. Javorka, Time irreversibility of heart rate oscillations during orthostasis,", Acta Med. Martiniana 11 (Supplement 1) (2011) 41–45.
[5] C.L. Ehlers, J. Havstad, D. Prichard, J. Theiler, Low doses of ethanol reduce evidence for nonlinear structure in brain activity, J. Neurosci. 18 (18) (1998) 7474–7486.
[6] P. Guzik, J. Piskorski, T. Krauze, A. Wykretowicz, H. Wysocki, Heart rate asymmetry by Poincaré plots of RR intervals, Biomedizinische Technik 51 (4) (2006) 272–275.
[7] M.D. Costa, C.-K. Peng, A.L. Goldberger, Multiscale analysis of heart rate dynamics: entropy and time irreversibility measures, Cardiovascular Engineering 8 (2) (2008) 88–93.
[8] A. Porta, G. D'addio, T. Bassani, R. Maestri, G.D. Pinna, Assessment of cardiovascular regulation through irreversibility analysis of heart period variability: a 24 hours Holter study in healthy and chronic heart failure populations,", Philos. Trans. Math. Phys. Eng. Sci. 367 (1892) (2009) 1359–1375.
[9] G.I. Choudhary, W. Aziz, I.R. Khan, S. Rahardja, P. Fränti, Analysing the dynamics of interbeat interval time series using grouped horizontal visibility graph, IEEE Access 7 (2019) 9926–9934.
[10] M. Costa, A.L. Goldberger, C.-K. Peng, Broken asymmetry of the human heartbeat: loss of time irreversibility in aging and disease,", Phys. Rev. Lett. 95 (19) (2005) 198102.
[11] W. Aziz, M. Rafique, I. Ahmad, M. Arif, N. Habib, M. Nadeem, Classification of heart rate signals of healthy and pathological subjects using threshold based symbolic entropy, Acta. Biol. Hung. 65 (3) (2014) 252–264.
[12] W. Aziz, M. Arif, Multiscale permutation entropy of physiological time series, 2005 Pakistan Section Multitopic Conference (2005) 1–6.
[13] J.N. Orellana, A.S. Sixto, B.D.L.C. Torres, E.S. Cachadiña, P.F. Martín, F.J.B. de la Rosa, Multiscale time irreversibility: Is it useful in the analysis of human gait? Biomed. Signal Process. Control 39 (2018) 431–434.
[14] D.R. Chialvo, M.M. Millonas, Asymmetric unbiased fluctuations are sufficient for the operation of a correlation ratchet,", Phys. Lett. A 209 (1–2) (1995) 26–30.
[15] M. Costa, A.L. Goldberger, C.-K. Peng, Multiscale entropy analysis of biological signals,", Phys. Rev. E 71 (2) (2005) 21906.
[16] A. Porta, S. Guzzetti, N. Montano, T. Gnecchi-Ruscone, R. Furlan, A. Malliani, Time Reversibility in Short-Term Heart Period Variability," 2006 Computers in Cardiology, 2006, pp. 77–80.
[17] A. Nuñez, L. Lacasa, E. Valero, J.P. Gómez, B. Luque, Detecting series periodicity with horizontal visibility graphs,", Int. J. Bifurc. Chaos 22 (07) (2012) 1250160.
[18] L. Lacasa, On the degree distribution of horizontal visibility graphs associated with Markov processes and dynamical systems: diagrammatic and variational approaches, Nonlinearity 27 (9) (2014) 2063.
[19] N. Pržulj, O. Kuchaiev, A. STEVANOVIĆ, W. Hayes, Geometric evolutionary dynamics of protein interaction networks, Biocomputing 2010, World Scientific (2010) 178–189.
[20] R. Flanagan, L. Lacasa, Irreversibility of financial time series: a graph-theoretical approach, Phys. Lett. A 380 (20) (2016) 1689–1697.
[21] J.H. Martínez, J.L. Herrera-Diestra, M. Chavez, Detection of time reversibility in time series by ordinal patterns analysis, Chaos Interdiscip. J. Nonlinear Sci. 28 (12) (2018) 123111.
[22] E. Sejdić, L.A. Lipsitz, Bio, Comput. Methods Programs Biomed. 111 (2) (2013) 459–470.
[23] M. Arif, W. Aziz, Application of threshold-based acceleration change index (TACI) in heart rate variability analysis, Physiol. Meas. 26 (5) (2005) 653.
[24] A.L. Goldberger, et al., PhysioBank, PhysioToolkit, and PhysioNet: components of a new research resource for complex physiologic signals, circulation 101 (23) (2000) e215–e220.
[25] NYHA, "New York Heart Association (NYHA) Classification." [Online], Available: [Accessed: 16-Oct-2019] https://manual.jointcommission.org/releases/TJC2016A/DataElem0439.html.
[26] B. Luque, L. Lacasa, F. Ballesteros, J. Luque, Horizontal visibility graphs: exact results for random time series, Phys. Rev. E 80 (4) (2009) 46103.
[27] J. Iacovacci, L. Lacasa, Sequential motif profile of natural visibility graphs, Phys. Rev. E 94 (5) (2016) 52309.
[28] L. Lacasa, A. Nunez, É. Roldán, J.M.R. Parrondo, B. Luque, Time series irreversibility: a visibility graph approach, Eur. Phys. J. B 85 (6) (2012) 217.
[29] L. Lacasa, B. Luque, F. Ballesteros, J. Luque, J.C. Nuno, From time series to complex networks: the visibility graph, Proc. Natl. Acad. Sci. 105 (13) (2008) 4972–4975.
[30] J.A. Hanley, B.J. McNeil, The meaning and use of the area under a receiver operating characteristic (ROC) curve, Radiology 143 (1) (1982) 29–36.
[31] I. Awan, et al., Studying the dynamics of interbeat interval time series of healthy and congestive heart failure subjects using scale based symbolic entropy analysis, PLoS One 13 (5) (2018) e0196823.